Available online at www.sciencedirect.com
SCIENCE DIRECT®
Chaos, Solitons and Fractals 26 (2005) 615–636
CHAOS SOLITONS & FRACTALS
www.elsevier.com/locate/chaos

Impulsive control and synchronization of spatiotemporal chaos ☆

Anmar Khadra [a,1], Xinzhi Liu [a,*], Xuemin Shen [b]

[a] Department of Applied Mathematics, University of Waterloo, Waterloo, ON, Canada N2L 3G1
[b] Department of Electrical and Computer Engineering, University of Waterloo, Waterloo, ON, Canada N2L 3G1

Accepted 10 January 2004

Communicated by Prof. Ji-Huaun He

Abstract

The impulsive control of spatiotemporal chaos of a particular type of non-linear partial differential equations has been investigated. A criterion for the solutions of these partial differential equations to be equi-attractive in the large is determined and an estimate for the basin of attraction is given in terms of the impulse durations and the magnitude of the impulses. Extending these results to impulsively synchronize spatiotemporal chaos of the same type of partial differential equations is explored. A proof for the existence of a certain kind of impulses for synchronization such that the error dynamics is equi-attractive in the large, is established. A comparison of the developed theoretical model with other existent numerical models available in the literature has been studied. Several simulation results are given to confirm the theoretical results. Moreover, an investigation of the Lyapunov exponents of the error dynamics between impulsively synchronized spatiotemporal chaotic systems, is done to further confirm the theoretical results.

1. Introduction

The theory of impulsive ordinary differential equations and its applications to the fields of science and engineering have been very active research topics [28–30,43–45], since the theory provides a natural framework for mathematical modeling of many physical phenomena. Furthermore, impulsive control, which is based on the theory of impulsive differential equations, has gained renewed interests recently for its promising applications towards controlling systems exhibiting chaotic behaviour. In fact, it was realized that, such a control method allows the stabilization of a chaotic system using only small control impulses, even though the chaotic behaviour may follow unpredictable patterns (in general, chaotic signals are broadband, noise like and difficult to predict). Examples include the impulsive control of autonomous systems of ODE's such as Lorenz system and Chua's oscillator [29,43,45] and non-autonomous chaotic systems

☆ Research supported by NSERC Canada.
* Corresponding author. Tel.: +1 519 888 4567x6007; fax: +1 519 746 4319.
E-mail address: xzliu@bbcr.uwaterloo.ca (X. Liu).
[1] Currently a postdoctoral fellow in the Department of Mathematics at the University of British Columbia.

0960-0779/$ - see front matter © 2005 Elsevier Ltd. All rights reserved.
doi:10.1016/j.chaos.2004.01.020

of ODE's, such as the Duffing's oscillator [42], where the stabilization of the chaotic system is achieved in a small region of the phase space using the notion of practical stability (instead of controlling the non-autonomous chaotic system to an equilibrium position).

One of the useful applications of impulsive control is the study of impulsive synchronization of two identical chaotic systems generated by ODE's. In [34,40,41,44], two autonomous chaotic ordinary differential systems, the drive system and the response system, have been considered for impulsive synchronization. Samples of the state variables of the drive system at discrete time instances are used to drive the response system. These samples are called the synchronization impulses and are employed to impulsively control the error system between the drive and the response systems. The asymptotic stability of the error dynamics is established, assuring the synchronization between the two systems, and an upper bound on the time intervals between the impulses is obtained. A generalization of this particular type of synchronization to time-varying impulse intervals has been further developed in [27], where less conservative conditions on the Lyapunov function are obtained in the sense that it is required to be non-increasing along a subsequence of the switching. The applications of impulsive synchronization to secure communications have been also developed [40,41]. Further detailed analysis of impulsive control and impulsive synchronization of chaotic systems are presented in [23,24,38,39].

Extending the theory of impulsive differential equations to partial differential equations has also gained considerable attention recently [1–3]. Several differential inequalities are obtained, and asymptotic stability results, comparison results and uniqueness results involving first order PDE's and first order partial differential-functional equations are established using the method of Lyapunov functions (also called energy functions for PDE's). In addition, numerical analysis of these first order partial differential equations is also investigated in [18]. This motivates the idea of generalizing the methods of impulsive control and impulsive synchronization to apply them on spatiotemporal chaotic systems generated by continuous extended systems. Early attempts of such approach include the synchronization of spatiotemporal chaotic systems generated by coupled non-linear oscillators (coupled non-linear ODE's) [20,22] and impulsive synchronization of spatiotemporal chaotic systems generated by PDE's [14,21,22]. Actually the idea of synchronizing partial differential equations, by applying other methods, such as synchronizing by means of a finite number of local tiny perturbations selected by an adaptive technique [4,5], or synchronizing by using an extended time-delay autosynchronization algorithm [8], or synchronizing by using only a finite number of coupling signals that are given in terms of local spatial averages (sensor coupling) [15,17,36], are some available methods for spatiotemporal synchronization in the literature. In fact some detailed study of frequency and phase synchronization of two non-identical PDE's has also been done in [5,16].

Due to the fact that the chaotic states in spatiotemporal systems, such as PDE's, are typically high dimensional, involving multiple stable and unstable modes, the idea of synchronization becomes a more challenging process when compared to synchronizing low dimensional chaotic systems produced by ODE's. For example, most of the coupling schemes for spatiotemporal synchronization, described earlier, are very difficult to implement experimentally because either the coupling has to be applied at all spatial points simultaneously or some variable of the driven system has to be reset to new values at specific points in space [17], unlike synchronizing ODE's. However, when impulsive synchronization is used, these two issues can be overcome since much smaller subset of points are driven impulsively in this method, as we shall explain later in this paper. Furthermore, another problem is associated with spatiotemporal synchronization: PDE's have inherently complex behaviour associated with them and that it takes them usually longer to be solved numerically when compared to ODE's, thus making synchronization a slow process. Although this might generate problems in implementation, it is believed, on the other hand, that this type of character for PDE's may lead to distinct advantages in masking information for secure communication (e.g., many more frequencies are involved in the mask when a PDE is used). In other words, this might make the transmission of information more secure. Therefore there has been several attempts to apply this theory to communication as a promising tool towards securing information transmission [9–11]. It was realized that [37] making multichannel (ten channels or a hundred channels, for instance) spread-spectrum communication by synchronizing spatiotemporal chaos, can greatly enhance the communication efficiency since a large number of informative signals can be transmitted and received simultaneously. It should be mentioned that employing impulsive synchronization of spatiotemporal chaos in secure communication remains currently under investigation to see how implementable this method can be.

Unfortunately, there has been no theoretical analysis of impulsive spatiotemporal synchronization to determine the type of conditions that the impulses must satisfy in order to achieve the desired property of synchronization. Furthermore, the analysis of the Lyapunov exponents of these models has not been yet explored. In order to entertain the idea of impulsive spatiotemporal synchronization between two continuous-time extended systems of PDE's, the notion of equi-attractivity in the large property [24] provides us with the required tool to investigate this type of synchronization theoretically. It gives the desired description needed to formulate the problem and set up the conditions on the different parameters of the systems together with the impulse durations and impulse magnitudes. This theoretical development

will give a solid mathematical explanation (which is not available in the literature) on how and why impulsive synchronization of spatiotemporal chaotic systems works, then we shall compare it with several numerical results known about this method of synchronization [21,22]. In addition, we shall confirm the theoretical results by developing a technique which analyzes the Lyapunov exponents of the error dynamics generated from the impulsive synchronization of these spatiotemporal chaotic systems. This technique is an extension of the method proposed by [13] which deals with systems of ODE's only. We shall generalize this technique to PDE's by incorporating it with the *numerical method of lines* [33], and then we shall generate a numerical result representing a sufficient condition for impulsive synchronization. The numerical result will be consistent with the results obtained from analyzing the same systems theoretically.

In this paper, we study the impulsive control of spatiotemporal chaos of one particular type of non-linear partial differential equations represented by the Kuramoto–Sivashinsky equation. Sufficient conditions to impulsively control the chaotic behaviour of the Kuramoto–Sivashinsky equation are derived to reflect upon the requirements to achieve its equi-attractivity in the large property. These conditions give an estimate on the basin of attraction in terms of the impulse durations and the magnitude of the impulses. Furthermore, we extend the result to impulsively synchronize two identical one-dimensional Grey–Scott models (Grey–Scott model is a reaction diffusion system). We prove the existence of a set of matrices Q_k, $k = 1,2,\ldots$, which guarantees that the error dynamics will be driven to zero, i.e., the solutions are equi-attractive in the large. We also provide a comparison between the theoretical development of this theory with the numerical analysis available in the literature by running simulations and by investigating the Lyapunov exponents. The rest of the paper is organized as follows. In Section 2, several classes of functions and definitions are stated. In Section 3, the impulsive control of the Kuramoto–Sivashinsky equation is studied with some examples. In Section 4, the impulsive synchronization of two identical Grey–Scott models is investigated and a numerical discussion is provided. Then in Section 5, the Lyapunov exponents of the error dynamics between two impulsively synchronized Grey–Scott models are analyzed. Finally, in Section 6, we give concluding remarks.

2. Preliminaries

Consider the impulsive initial boundary value problem presented by the one-dimensional (i.e., one spatial dimension) n^{th} order partial differential equation given by

$$\left\{\begin{array}{l} \left.\begin{array}{ll} \frac{\partial \mathbf{u}}{\partial t} = \mathbf{f}\left(t,x,\mathbf{u},\frac{\partial \mathbf{u}}{\partial x},\frac{\partial^2 \mathbf{u}}{\partial x^2},\ldots,\frac{\partial^n \mathbf{u}}{\partial x^n}\right) & t \neq t_k, \\ \Delta\mathbf{u}(t,x) = Q_k\mathbf{u}(t,x), & t = t_k \end{array}\right\} \quad t \in \mathbb{R}_+, k = 1,2,\ldots, \\ \mathbf{u}(0^+,x) = \mathbf{u}_0(x), \quad x \in [0,L], \\ \mathbf{u}(t,0) = \mathbf{u}(t,L) = \mathbf{h}_1(t), \quad t \in \mathbb{R}_+, \\ \frac{\partial \mathbf{u}}{\partial x}(t,0) = \frac{\partial \mathbf{u}}{\partial x}(t,L) = \mathbf{h}_2(t), \quad t \in \mathbb{R}_+, \\ \vdots \\ \frac{\partial^{n_1}\mathbf{u}}{\partial x^{n_1}}(t,0) = \frac{\partial^{n_1}\mathbf{u}}{\partial x^{n_1}}(t,L) = \mathbf{h}_{n_1}(t), \quad t \in \mathbb{R}_+ \end{array}\right. \tag{1}$$

for some $n_1 \geqslant 0$, where

$$\frac{\partial \mathbf{u}}{\partial t} = \left(\frac{\partial u_1}{\partial t},\frac{\partial u_2}{\partial t},\ldots,\frac{\partial u_m}{\partial t}\right)^{\mathrm{T}},$$
$$\frac{\partial \mathbf{u}}{\partial x} = \left(\frac{\partial u_1}{\partial x},\frac{\partial u_2}{\partial x},\ldots,\frac{\partial u_m}{\partial x}\right)^{\mathrm{T}},$$
$$\frac{\partial^2 \mathbf{u}}{\partial x^2} = \left(\frac{\partial^2 u_1}{\partial x^2},\frac{\partial^2 u_2}{\partial x^2},\ldots,\frac{\partial^2 u_m}{\partial x^2}\right)^{\mathrm{T}},$$
$$\vdots$$
$$\frac{\partial^n \mathbf{u}}{\partial x^n} = \left(\frac{\partial^n u_1}{\partial x^n},\frac{\partial^n u_2}{\partial x^n},\ldots,\frac{\partial^n u_m}{\partial x^n}\right)^{\mathrm{T}},$$

$\Delta\mathbf{u}(t_k,x) := \mathbf{u}(t_k^+,x) - \mathbf{u}(t_k^-,x)$, for all $x \in [0,L]$, $\mathbf{u}(t_k^+,x) = \lim_{t\to t_k^+}\mathbf{u}(t,x)$, for a fixed $x \in [0,L]$, and the moments of impulse satisfy $0 = t_1 < t_2 < \cdots < t_k < \cdots$ and $\lim_{k\to\infty} t_k = \infty$. The matrices Q_k are $m \times m$ constant matrices satisfying $\|Q_k\| := \sqrt{\lambda_{\max}(Q_k^{\mathrm{T}}Q_k)} < L_1$, for every $k = 1,2,\ldots$ and some $L_1 > 0$ ($\lambda_{\max}(Q^{\mathrm{T}}Q)$ is the largest eigenvalue of Q^{T} Q).

Let $\mathbf{f}:\mathbb{R}_+\times[0,L]\times\mathbb{R}^m\times\cdots\to\mathbb{R}^m$ be continuous on $(t_k,t_{k+1}]\times[0,L]\times\mathbb{R}^m\times\cdots\to\mathbb{R}^m$, and $\mathbf{f}(t_k^+,x,\mathbf{u},\partial\mathbf{u}/\partial x,\partial^2\mathbf{u}/\partial x^2,\ldots,\partial^n\mathbf{u}/\partial x^n)$ exist for every $k=1,2,\ldots$ Let $n=2$ in the above model and assume that $\mathbf{f}$ satisfies Lipschitz condition with respect to $\mathbf{u}$, $\partial\mathbf{u}/\partial x$ and $\partial^2\mathbf{u}/\partial x^2$. Furthermore, assume that there exist functions $\mathbf{f}_1(t,\mathbf{u})$ and $\mathbf{f}_2(t,\mathbf{u})$ such that

$$\mathbf{f}_1(t,\mathbf{u})\leqslant\mathbf{f}(t,x,\mathbf{u},\mathbf{0},\mathbf{0})\leqslant\mathbf{f}_2(t,\mathbf{u})$$

for every $(t,x,\mathbf{u})\in[0,T]\times[0,L]\times\mathbb{R}^m$, where the inequality holds componentwise and T is a positive number, and that there exist solutions $\boldsymbol{\gamma}(t)$ and $\boldsymbol{\rho}(t)$ to the systems given by

$$\begin{cases}\dot{\boldsymbol{\gamma}}(t)=\mathbf{f}_1(t,\boldsymbol{\gamma}),\quad t\neq 0,t_k,T,\quad 1\leqslant k\leqslant m_1,\\ \Delta\boldsymbol{\gamma}(t_k)=Q_k\boldsymbol{\gamma}(t_k),\quad 1\leqslant k\leqslant m_1,\\ \boldsymbol{\gamma}(0^+)=\boldsymbol{\gamma}_0\end{cases}$$

and

$$\begin{cases}\dot{\boldsymbol{\rho}}(t)=\mathbf{f}_2(t,\boldsymbol{\rho}),\quad t\neq 0,\ t_k,T,\quad 1\leqslant k\leqslant m_1,\\ \Delta\boldsymbol{\rho}(t_k)=Q_k\boldsymbol{\rho}(t_k),\quad 1\leqslant k\leqslant m_1,\\ \boldsymbol{\rho}(0^+)=\boldsymbol{\rho}_0,\end{cases}$$

respectively, where $t_{m_1}\leqslant T$. If $\boldsymbol{\rho}_0\leqslant\boldsymbol{u}_0(x)\leqslant\boldsymbol{\gamma}_0$ on $[0,L]$ and if there exists a function $p\in C((0,T)\times\{0,L\},\mathbb{R}_+)$, such that, for $i=1,\ldots,n_1$,

$$p(t,x)\boldsymbol{\rho}(t)\leqslant\mathbf{h}_i(t)\leqslant p(t,x)\boldsymbol{\gamma}(t),$$

$t\neq t_k$, $k=1,2,\ldots,m_1$, then there exists a local solution $\mathbf{u}(t,x)$ for system (1) satisfying

$$\boldsymbol{\rho}(t)\leqslant\mathbf{u}(t,x)\leqslant\boldsymbol{\gamma}(t)$$

provided that the original partial differential equation, in (1), without the impulses, has a solution [7]. For $x\in[0,L]$, let $\mathbf{u}(t,x):=\mathbf{u}(t,x,\mathbf{u}_0(x))$ be any solution of (1) satisfying $\mathbf{u}(0^+,x)=\mathbf{u}_0(x)$ and $\mathbf{u}(t,x)$ be left continuous at each $t_k>0$, $k=1,2,\ldots$, in its interval of existence, i.e., $\mathbf{u}(t_k^-,x)=\mathbf{u}(t_k,x)$, for every $x\in[0,L]$.

Definition 1. Suppose that $\mathbf{u}(t,x):\mathbb{R}_+\times[0,L]\to\mathbb{R}^m$ for some $m>0$, where $\mathbf{u}$ is of class $\mathscr{L}_2[0,L]$ with respect to x. Then $\|\cdot\|_2$ of $\mathbf{u}(t,x)$ is defined by

$$\|\mathbf{u}(t,x)\|_2:=\left\{\int_0^L\|\mathbf{u}(t,x)\|^2\,\mathrm{d}x\right\}^{1/2},$$

where $\|\cdot\|$ is the Euclidean norm. In order to study the dynamics of particular systems whose structures resemble system (1), we shall introduce the following classes of functions and definitions. Let

$$\begin{aligned}&S^c(M):=\{\mathbf{u}\in\mathbb{R}^m:\|\mathbf{u}\|_2\geqslant M\},\\ &S^c(M)^0:=\{\mathbf{u}\in\mathbb{R}^m:\|\mathbf{u}\|_2>M\},\\ &v_0(M):=\{V:\mathbb{R}_+\times S^c(M)\to\mathbb{R}_+:V(t,\mathbf{u})\in C((t_k,t_{k+1}]\times S^c(M)),\ \text{locally Lipschitz in }\mathbf{u}\text{ and }V(t_k^+,\mathbf{u})\\ &\text{exists for }k=1,2,\ldots\},\ \text{where } M\geqslant 0.\end{aligned}$$

Definition 2. Let $M\geqslant 0$ and $V\in v_0(M)$. Define the upper right derivative of $V(t,\mathbf{u})$ with respect to the continuous portion of system (1), for $(t,\mathbf{u})\in\mathbb{R}_+\times S^c(M)^0$ and $t\neq t_k$, $k=1,2,\ldots$, by

$$D_t^+V(t,\mathbf{u}):=\lim_{\delta\to 0^+}\sup\frac{1}{\delta}\left[V\left(t+\delta,\mathbf{u}+\delta\mathbf{f}\left(t,x,\mathbf{u},\frac{\partial\mathbf{u}}{\partial x},\frac{\partial^2\mathbf{u}}{\partial x^2},\ldots,\frac{\partial^n\mathbf{u}}{\partial x^n}\right)\right)-V(t,\mathbf{u})\right].$$

Definition 3. Solutions of the impulsive system (1) are said to be

(S1) equi-attractive in the large if for each $\epsilon>0$, $\alpha>0$ and $t_0\in\mathbb{R}_+$, there exists a number $T:=T(t_0,\epsilon,\alpha)>0$ such that $\|\mathbf{u}(t_0,x)\|_2<\alpha$ implies $\|\mathbf{u}(t,x)\|_2<\epsilon$, for $t\geqslant t_0+T$;
(S2) uniformly equi-attractive in the large if T in (S1) is independent of t_0.

From the definition of equi-attractivity in the large, it can been seen that the solutions of system (1), which possess this property, will converge to zero, with respect to the $\|\cdot\|_2$, no matter how large $\|\mathbf{u}(t_0,x)\|_2$ is. In other words, $\lim_{t\to\infty}\|\mathbf{u}(t,x)\|_2=0$. Moreover, the properties (S1) and (S2) in Definition 3 become identical for autonomous systems

[24], i.e., when $\mathbf{f}(t,x,\mathbf{u},\partial\mathbf{u}/\partial x,\ldots,\partial^n\mathbf{u}/\partial x^n)=\mathbf{f}(x,\mathbf{u},\partial\mathbf{u}/\partial x,\ldots,\partial^n\mathbf{u}/\partial x^n)$. Therefore when dealing with autonomous systems, the uniform terminology will be automatically removed.

The above definitions will be used heavily in exploring the conditions under which the solutions generated by several impulsive PDE's are equi-attractive in the large. We begin by discussing the impulsive control of the Kuramoto–Sivashinsky equation.

3. Impulsive control of the Kuramoto–Sivashinsky equation

Consider the impulsive control of the Kuramoto–Sivashinsky equation represented by the impulsive initial boundary value problem given by

$$\begin{cases} \left.\begin{array}{ll} u_t+(u^2)_x+u_{xx}+u_{xxxx}=0, & t\neq t_k \\ \Delta u(t,x)=-q_k u(t,x), & t=t_k, \end{array}\right\} \quad t\in\mathbb{R}_+,\ k=1,2,\ldots, \\ u(0,x)=u_0(x), \quad x\in[0,L], \\ u(t,0)=u(t,L)=0, \quad t\in\mathbb{R}_+, \\ u_x(t,0)=u_x(t,L)=0, \quad t\in\mathbb{R}_+, \end{cases} \tag{2}$$

where $q_k>0, k=1,2,\ldots$, and L is the only free parameter. Eq. (2), with the absence of the impulses, exhibits extensive chaos, which means that the Lyapunov dimension of the attractor grows linearly with the system size L [6], as shown in Fig. 1.

The following lemma gives upper bounds on $\|u(t,x)\|_2$ and $\|u_x(t,x)\|_2$ in terms of $\|u_{xx}(t,x)\|_2$. This lemma is the well-known Poincaré inequality described in [31,35].

Lemma 1. *Let* $J=[0,L]$ *and* $u\in C^2(J)$. *If* $u(0)=u(L)=0$, *then*

$$\|u(x)\|_2\leqslant\frac{L}{\pi}\|u_x(x)\|_2. \tag{3}$$

The next Theorem gives the required criteria for system (2) to be equi-attractive in the large. It provides us with a tool towards impulsively controlling the chaotic behaviour of the Kuramoto–Sivashinsky equation by forcing the solution to converge to zero.

Theorem 1. *Let* $q=\min_k q_k$ *and* $\Delta_{k+1}=t_{k+1}-t_k\leqslant\Delta$, *for* $k=1,2,\ldots$ *and for some* $\Delta>0$. *Then the impulsive Kuramoto–Sivashinsky Eq. (2) is equi-attractive in the large if*

$$(1-q)^2e^{\zeta\Delta}<1, \tag{4}$$

where $\zeta=1-(\pi/L)^4$.

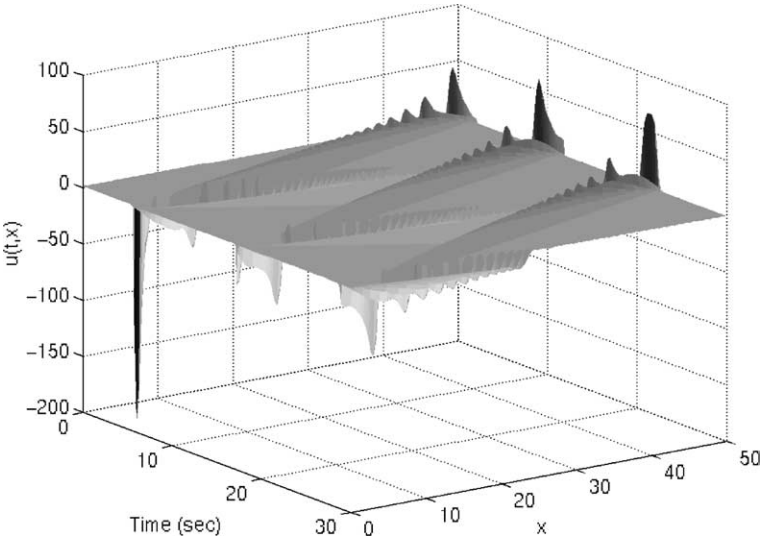

Fig. 1. Propagation of the solution of the Kuramoto–Sivashinsky equation without the impulses.

Proof. We shall prove this theorem by choosing an appropriate Lyapunov function $V(u(t,x))$. Let

$$V(u(t,x)) := \|u(t,x)\|_2^2 = \int_0^L u(t,x)^2\,\mathrm{d}x.$$

Then, by system (2) with its boundary conditions, by Definition 2 and by applying integration by parts, we obtain, for all $t \in (t_k, t_{k+1}]$, $k = 1,2,\ldots,$

$$\begin{aligned} D_t^+ V(u(t,x)) &= \int_0^L 2u(t,x)u_t(t,x)\mathrm{d}x = \int_0^L (-4u(t,x)^2u_x(t,x) - 2u(t,x)u_{xx}(t,x) - 2u(t,x)u_{xxxx}(t,x))\mathrm{d}x \\ &= -\frac{4}{3}u(t,x)^3\Big|_0^L - 2\int_0^L u(t,x)u_{xx}(t,x)\mathrm{d}x - 2u(t,x)u_{xxx}(t,x)\Big|_0^L + 2u_x(t,x)u_{xx}(t,x)\Big|_0^L - 2\int_0^L u_{xx}(t,x)^2\mathrm{d}x \\ &= -2\int_0^L u(t,x)u_{xx}(t,x)\mathrm{d}x - 2\int_0^L u_{xx}(t,x)^2\mathrm{d}x \leqslant \int_0^L u(t,x)^2\mathrm{d}x + \int_0^L u_{xx}(t,x)^2\mathrm{d}x - 2\int_0^L u_{xx}(t,x)^2\mathrm{d}x \\ &= \|u(t,x)\|_2^2 - \|u_{xx}(t,x)\|_2^2. \end{aligned}$$

However, by Lemma 1, we have

$$\|u(t,x)\|_2^2 \leqslant L^2/\pi^2\|u_x(t,x)\|_2^2.$$

Since $u_x(t,x)$ satisfies the conditions of Lemma 1, we have once more

$$\|u_x(t,x)\|_2^2 \leqslant L^2/\pi^2\|u_{xx}(t,x)\|_2^2.$$

Thus

$$D_t^+ V(u(t,x)) \leqslant \|u(t,x)\|_2^2 - \frac{\pi^4}{L^4}\|u(t,x))\|_2^2 = \zeta V(u(t,x)).$$

Hence, for all $t \in (t_k, t_{k+1}]$, $k = 1,2,\ldots,$ we have

$$V(u(t,x)) \leqslant \mathrm{e}^{\zeta(t-t_k)}V(u(t_k^+,x)) \tag{5}$$

and

$$V(u(t_{k+1},x)) \leqslant \mathrm{e}^{\zeta\Delta_{k+1}}V(u(t_k^+,x)). \tag{6}$$

Moreover, according to the structure of the impulses defined in (2), we have, for all $x \in [0,L]$ and $k = 1,2,\ldots,$

$$u(t_k^+,x) = u(t_k,x) - q_k u(t_k,x) = (1-q_k)u(t_k,x) \Rightarrow \int_0^L u(t_k^+,x)^2\,\mathrm{d}x = \int_0^L (1-q_k)^2 u(t_k,x)^2\,\mathrm{d}x.$$

It follows that

$$V(u(t_k^+,x)) = (1-q_k)^2 V(u(t_k,x)). \tag{7}$$

Hence, by using inequalities (6) and (7), we have, for every $k = 1,2,\ldots,$

$$V(u(t_{k+1},x)) \leqslant (1-q_k)^2\mathrm{e}^{\zeta\Delta_{k+1}}V(u(t_k,x)) \leqslant (1-q)^2\mathrm{e}^{\zeta\Delta}V(u(t_k,x)). \tag{8}$$

By inequalities (4) and (8), we can conclude that

$$\lim_{k\to\infty} V(u(t_k,x)) = 0.$$

Therefore, by inequality (5), we have, for all $t \in (t_k, t_{k+1}]$ and $k = 1,2,\ldots,$

$$V(u(t,x)) \leqslant \mathrm{e}^{\zeta\Delta_{k+1}}V(u(t_k^+,x)) \leqslant (1-q_k)^2\mathrm{e}^{\zeta\Delta_{k+1}}V(u(t_k,x)) \leqslant (1-q)^2\mathrm{e}^{\zeta\Delta}V(u(t_k,x)) \to 0, \quad \text{as } k \to \infty.$$

It follows that

$$\lim_{t\to\infty} V(u(t,x)) = 0.$$

In other words the solutions to the impulsive Kuramoto–Sivashinsky equation, defined by (2), are equi-attractive in the large. □

Remark 1. From Theorem 1, we see the spatiotemporal chaotic behaviour (or when $\pi/L \ll 1$) of the Kuramoto–Sivashinsky equation, described by the partial differential equation in (2), is impulsively controlled and the solutions are driven towards the equilibrium solution $u(t,x) = 0$, achieving the desired equi-attractivity property. The proof is done by reducing the problem from a PDE problem into an ODE involving the Lyapunov function $V(u(t,x))$ which is easier to handle.

Remark 2. From the proof of Theorem 1, it is concluded that if the ratio π/L is chosen to be strictly greater than 1 (by taking smaller spatial range L), the solutions of the Kuramoto–Sivashinsky equation will remain equi-attractive in the large even with the absence of the impulses. A numerical example showing this phenomenon will be given in this section. However, if $\pi/L < 1$, then the impulses are needed to stabilize the system provided that these impulses satisfy the condition stated in Theorem 1.

Remark 3. The condition in Theorem 1 is a sufficient condition but not necessary. In other words, the impulsive partial differential equation described by system (2) may remain equi-attractive in the large even if inequality (4) is not satisfied. We shall demonstrate this result in the numerical example given in this section.

Remark 4. Inequality (4) reflects the type of relationship that exists between the magnitude of the impulses (represented by the parameter q) and the duration of the impulses (represented by the parameter Δ). Thus the larger the impulse duration Δ_k is, the stronger the magnitude of the impulse q_k, for all $k \geqslant K$ for some $K \geqslant 1$, is required to maintain the equi-attractivity property (see Fig. 2). An estimate on the basin of attraction can be obtained by solving for Δ:

$$\Delta < \Delta_{\max} = \frac{-\ln(1-q)^2}{\zeta}, \quad \text{for } 0 < q < 2.$$

The following numerical examples illustrate Theorem 1 and Remarks 1–4. When $L = 50$, the Kuramoto–Sivashinsky equation, given in (2), exhibits chaotic behaviour in both time and space. If we take the magnitude of the impulses to be $q_k = q = 0.4$, for all $k = 1, 2, \ldots$, then Theorem 1 indicates that the maximum impulse duration permissible to guarantee the equi-attractivity property (i.e., convergence to the equilibrium solution) is given by $\Delta_{\max} \approx 1.022$ s. In other words, if the impulse durations satisfy $\Delta_k < \Delta_{\max}$, $k = 1, 2, \ldots$, then $\lim_{t\to\infty} \|u(t,x)\|_2 = 0$. This can be shown in Fig. 3, where the time of the convergence is approximately 0.12 s. In this numerical simulation and the remaining ones in this section, a MacCormack's method [25,26], with first forward differencing and then backward differencing to achieve second order accuracy, is applied. The time step size is taken to be 0.0001 s and the number of spatial points is taken to be 150. Moreover, in all of these simulations, the initial condition is taken to be $u_0(x) = 0$ with strong perturbations in the middle. Increasing the magnitude of the impulses to $q_k = q = 0.7$, $k = 1, 2, \ldots$, the maximum impulse duration predicted by Theorem 1 becomes $\Delta_{\max} = 2.408$ s Fig. 4 shows the convergence of $\|u(t,x)\|_2$ to zero with impulse duration $\Delta_k = \Delta = 0.1$ s, for $k = 1, 2, \ldots$, which is consistent with that of Theorem 1. This illustrates the type of relationship that exists between the impulse durations and the magnitude of the impulses, as mentioned in Remark 4. Furthermore, when applying

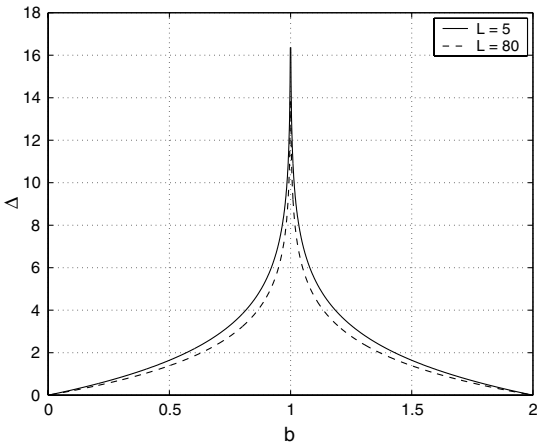

Fig. 2. Basin of attraction of Δ with respect to q for different values of L.

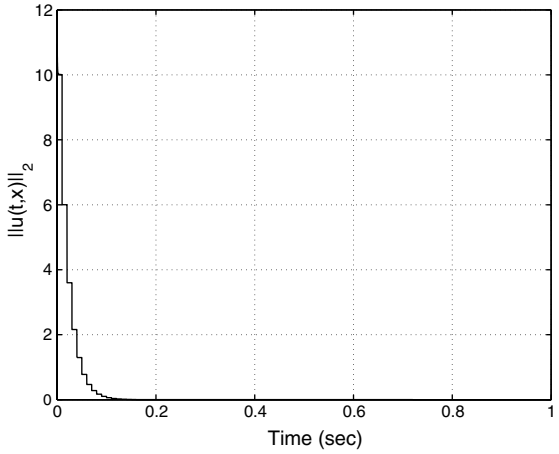

Fig. 3. $\|u(t,x)\|_2$ converging to zero for $\Delta = 0.01$, $q_k = q = 0.4$ and $L = 50$.

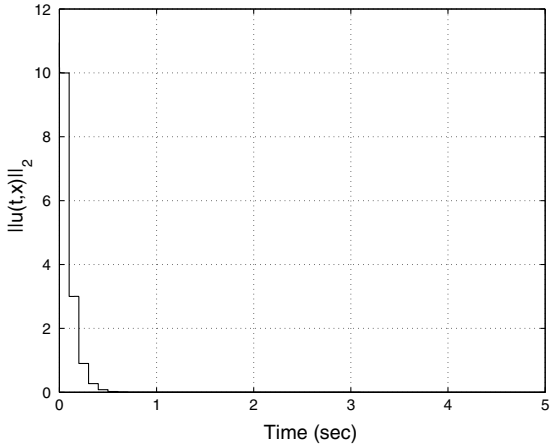

Fig. 4. $\|u(t,x)\|_2$ converging to zero for $\Delta = 0.1$, $q_k = q = 0.7$ and $L = 50$.

impulses with magnitude $q_k = q = 0.2$, $k = 1, 2, \ldots, \Delta_{\max} = 0.4463$ s, according to Theorem 1, and the impulsive control of the Kuramoto–Sivashinsky equation can still be achieved with impulse durations given by $\Delta_k = \Delta = 0.45 > \Delta_{\max}$ (see Fig. 5). This indicates that condition (4), in Theorem 1, is a sufficient condition but not necessary, as we discussed in Remark 3. In other words, the equi-attractivity property was still achieved even if the impulses lie outside the basin of attraction described by Fig. 2. However, if these impulses lie drastically far from the basin of attraction, then the solutions to system (2) will not converge to zero, as shown in Fig. 6, where $\Delta_k = \Delta = 1 > \Delta_{\max}$. Finally, we show in Fig. 7, the convergence of the solutions of the Kuramoto–Sivashinsky equation to zero without the impulses because $L = 2$ and $(\pi/L) < 1$, as was mentioned in Remark 2.

4. Impulsive synchronization of the Grey–Scott model

We have been successful in using impulsive control methods to control the behaviour of the Kuramoto–Sivashinsky equation by making its solutions equi-attractive in the large, although the original PDE exhibited spatiotemporal chaotic behaviour. We will extend this work and investigate the impulsive synchronization of two identical spatiotemporal chaotic systems. The Grey–Scott model [32] will be used as the spatiotemporal chaos generator. The coming theory is definitely applicable to the synchronization of two Kuramoto–Sivashinsky equations as well as any other spatiotemporal chaotic system exhibiting the same structure.

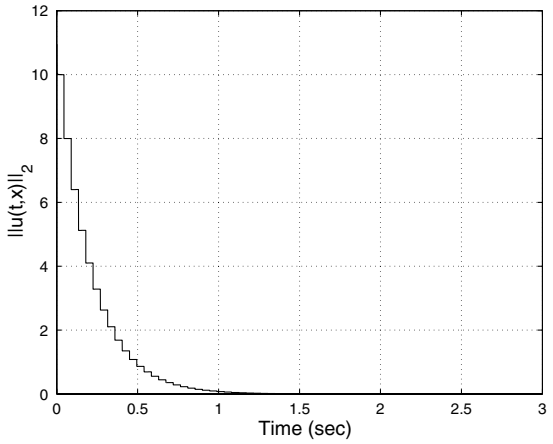

Fig. 5. $\|u(t,x)\|_2$ converging to zero for $\Delta = 0.45$, $q_k = q = 0.2$ and $L = 50$.

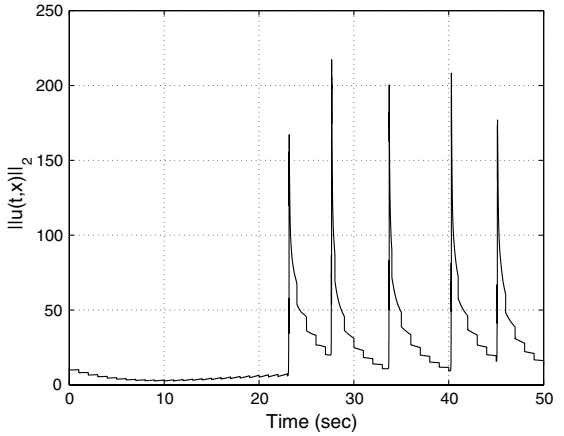

Fig. 6. $\|u(t,x)\|_2$ not converging to zero for $\Delta = 1$, $q_k = q = 0.2$ and $L = 50$.

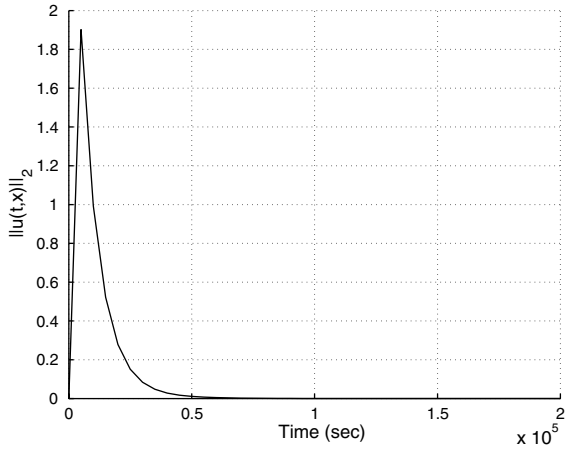

Fig. 7. $\|u(t,x)\|_2$ converging without the presence of impulses for $L = 2$.

The Grey–Scott cubic auto-catalysis model is a reaction–diffusion system which corresponds to two reactions which are both irreversible. This model exhibits mixed mode spatiotemporal chaos and is described by the following equations.

$$\begin{aligned}\frac{\partial u_1}{\partial t} &= -u_1u_2^2 + a(1-u_1) + d_1\nabla^2 u_1,\\ \frac{\partial u_2}{\partial t} &= u_1u_2^2 - (a+b)u_2 + d_2\nabla^2 u_2,\end{aligned} \tag{9}$$

where b is the dimensionless rate constant of the second reaction, a is the dimensionless feed rate and d_1 and d_2 are the diffusion coefficients. The system size is 2.5×2.5 and the boundary conditions are periodic. Detailed stability and bifurcation analysis of the above model is given in [32]. Figs. 8 and 9 show the propagation of the solutions $u_1(t,x)$ and $u_2(t,x)$ for the one-dimensional case. A forward Euler integration of the finite difference equation, resulting from the discretization of the diffusion operator, is applied with 257 mesh points and 0.01 integration step size. The initial con-

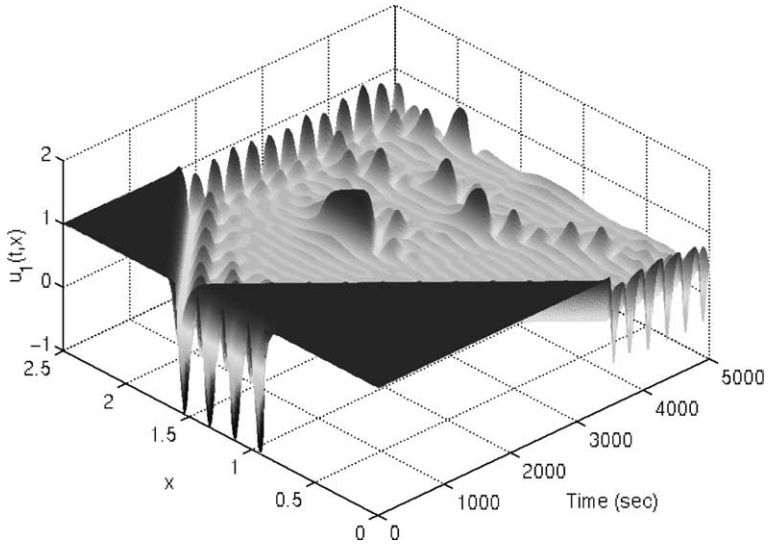

Fig. 8. Propagation of $u_1(t,x)$ in the one-dimensional case for Eq. (9).

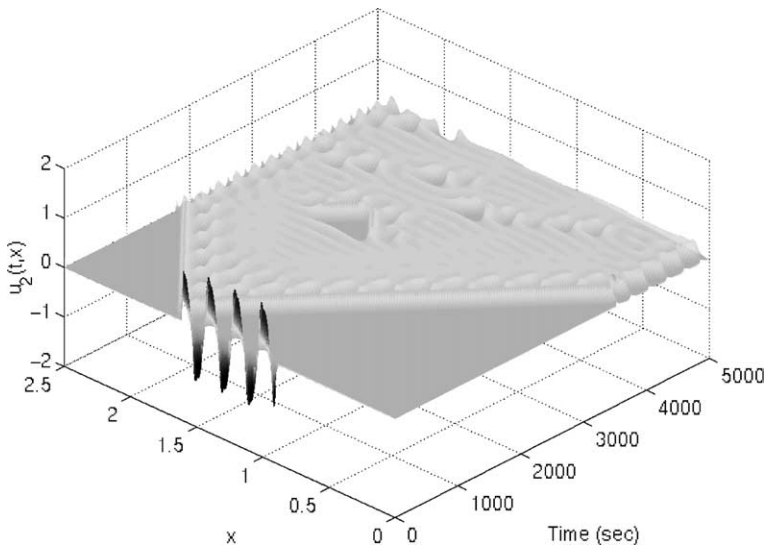

Fig. 9. Propagation of $u_2(t,x)$ in the one-dimensional case for Eq. (9).

ditions are chosen to be $(u_{01}, u_{02})^{\mathrm{T}} = (1,0)^{\mathrm{T}}$ with strong perturbations in the middle and the parameters of the system are taken to be $a = 0.028$, $b = 0.053$, $d_1 = 2\times 10^{-5}$ and $d_2 = 10^{-5}$. In the following, we shall discuss the impulsive synchronization of the one-dimensional version of this system with another identical system starting from different initial conditions. In other words, we investigate the synchronization of the chaotic signal $\mathbf{u}(t,x) = (u_1(t,x), u_2(t,x))^{\mathrm{T}}$, given by

$$\text{Transmitter:}\quad \begin{cases} \left.\begin{aligned} \tfrac{\partial u_1}{\partial t} &= -u_1u_2^2 + a(1-u_1) + d_1\tfrac{\partial^2 u_1}{\partial x^2} \\ \tfrac{\partial u_2}{\partial t} &= u_1u_2^2 - (a+b)u_2 + d_2\tfrac{\partial^2 u_2}{\partial x^2} \end{aligned}\right\} & t\in\mathbb{R}_+, \\ \mathbf{u}(0,x) = \mathbf{u}_0(x), \quad x\in[0,L], \\ \mathbf{u}(t,0) = \mathbf{u}(t,L) = \mathbf{h}(t), \quad t\in\mathbb{R}_+, \end{cases} \tag{10}$$

with the chaotic signal $\mathbf{v}(t,x) = (v_1(t,x), v_2(t,x))^{\mathrm{T}}$, given by

$$\text{Receiver:}\quad \begin{cases} \left.\begin{aligned} \tfrac{\partial v_1}{\partial t} &= -v_1v_2^2 + a(1-v_1) + d_1\tfrac{\partial^2 v_1}{\partial x^2} \\ \tfrac{\partial v_2}{\partial t} &= v_1v_2^2 - (a+b)v_2 + d_2\tfrac{\partial^2 v_2}{\partial x^2} \end{aligned}\right\} & t\neq t_k,\ \ k=1,2,\ldots, \\ \Delta\mathbf{v}(t,x) = -Q_k\mathbf{e}(t,x), \quad t=t_k, \quad x\in[0,L],\ \ k=1,2,\ldots, \\ \mathbf{v}(0,x) = \mathbf{v}_0(x), \quad x\in[0,L], \\ \mathbf{v}(t,0) = \mathbf{v}(t,L) = \tilde{\mathbf{h}}(t), \quad t\in\mathbb{R}_+, \end{cases} \tag{11}$$

where a, b, d_1 and d_2 are as defined before, $L = 2.5$ is the linear extension of the reactor tank, $\mathbf{u}_0(x)$ and $\mathbf{v}_0(x)$ are the initial conditions, $\mathbf{h}(t)$ is the periodic boundary condition for the transmitter system, $\mathbf{e}(t,x) := \mathbf{u}(t,x) - \mathbf{v}(t,x)$. Q_k are 2×2 constant matrices satisfying $\|Q_k\| < L_1$, for every $k = 1,2,\ldots$ and some $L_1 > 0$. The boundary condition $\tilde{\mathbf{h}}(t)$ described at the receiver, is defined by

$$\tilde{\mathbf{h}}(t) := \mathbf{h}(t) - \mathbf{g}(t)\left\{1 + \sum_{k=1}^{\infty}\left[(\|I+Q_k\|^{2k} - \|I+Q_{k-1}\|^{2(k-1)})H(t-t_k)\right]\right\}, \tag{12}$$

where $\mathbf{g}(t) = (g_1(t), g_2(t))^{\mathrm{T}} \in C^1(\mathbb{R}_+)$, $\|\mathbf{g}(t)\| \leqslant N$, for some $N > 0$ and for all $t\in\mathbb{R}_+$, I is the 2×2 identity matrix, Q_0 is defined to be the zero matrix (i.e., $Q_0 = 0$) and $H(t-t_k)$, $k = 1,2,\ldots$, is the alternative heaviside step function defined by

$$H(t-t_k) = \begin{cases} 0 & \text{if } t\leqslant t_k, \\ 1 & \text{if } t > t_k. \end{cases}$$

According to Eqs. (10)–(12), the error system $\mathbf{e}(t,x)$ will be given by

$$\begin{cases} \left.\begin{aligned} \tfrac{\partial e_1}{\partial t} &= -u_1u_2^2 + v_1v_2^2 - ae_1 + d_1\tfrac{\partial^2 e_1}{\partial x^2} \\ \tfrac{\partial e_2}{\partial t} &= u_1u_2^2 - v_1v_2^2 - (a+b)e_2 + d_2\tfrac{\partial^2 e_2}{\partial x^2} \end{aligned}\right\} & t\neq t_k, \quad k=1,2,\ldots, \\ \Delta\mathbf{e}(t,x) = Q_k\mathbf{e}(t,x), \quad t=t_k, \quad x\in[0,L],\ \ k=1,2,\ldots, \\ \mathbf{e}(0,x) = \mathbf{e}_0(x), \quad x\in[0,L], \\ \mathbf{e}(t,0) = \mathbf{e}(t,L) = \widetilde{\mathbf{H}}(t), \quad t\in\mathbb{R}_+, \end{cases} \tag{13}$$

where $\mathbf{e}_0(t) := \mathbf{u}_0(t) - \mathbf{v}_0(t)$ and

$$\widetilde{\mathbf{H}}(t) := \mathbf{g}(t)\left\{1 + \sum_{k=1}^{\infty}\left[(\|I+Q_k\|^{2k} - \|I+Q_{k-1}\|^{2(k-1)})H(t-t_k)\right]\right\}.$$

Notice that if $\|I+Q_k\| \leqslant L_2 < 1$, for every $k = 1,2,\ldots$, then

$$\lim_{t\to\infty}\|\widetilde{\mathbf{H}}(t)\| = \lim_{t\to\infty}\|\mathbf{h}(t) - \tilde{\mathbf{h}}(t)\| = 0.$$

This is a very important property which will be used in the upcoming theory. Furthermore, Due to the fact that $\mathbf{u}$ and $\mathbf{v}$ are both generated by spatiotemporal chaotic systems, we may conclude immediately that they are both equi-bounded [24]. This will also be a very useful property which will be used in the proof of the next theorem. Thus, using the above description, to explore the idea of impulsively synchronizing the two systems $\mathbf{u}$ and $\mathbf{v}$, reduces to proving that the error system (13) is equi-attractive in the large or that $\lim_{t\to\infty}\|\mathbf{e}(t,x)\|_2 = 0$.

We shall state now two lemmas ([19], Theorem 3.1, p. 45 and Corollary 2.2, p 33, respectively) and prove two other ones in order to establish several results needed in obtaining certain criteria for system (13) to be equi-attractive in the large.

Lemma 2. *Let $p(t) \neq 0$ and $r(t)$ be given functions for $t = \ell, \ell+1, \ell+2, \ldots$, for some $\ell \in \mathbb{R}_+ \cup \{0\}$. Then*

(a) *The solutions of the equation $w(t+1) = p(t)w(t)$ are given by*

$$w(t) = w(\ell)\prod_{s=\ell}^{t-1} p(s).$$

(b) *All solutions of the equation $z(t+1) = p(t)z(t) + r(t)$ are given by*

$$z(t) = w(t)\left[\sum \frac{r(t)}{Ew(t)} + C\right],$$

where $\sum$ is the indefinite sum, E is the shift operator ($Ez(t) = z(t+1)$), C is an arbitrary constant and $w(t)$ is any non-zero solution from part (a).

Lemma 3. *If $n \in \mathbb{Z}_+ \cup \{0\}$, than*

$$\sum t^n = \frac{1}{1+n}B_{n+1}(t) + C,$$

where B_n are Bernoulli polynomials [19], for all $n \in \mathbb{Z}_+ \cup \{0\}$, and C is an arbitrary constant.

Lemma 4. *Let $p(t) := q$ and $r(t) := Kt^n q^{t-1}$ in Lemma 2, for all $t = 1, 2, \ldots (\ell = 1)$, where $0 < q < 1$, $n \in \mathbb{Z}_+ \cup \{0\}$ and $K \in \mathbb{R}_+$. Then $\lim_{t\to\infty} z(t) = 0$.*

Proof. From Lemmas 2 and 3, we can conclude that $w(t) = q^t w(1)$ and

$$\begin{aligned} z(t) &= w(t)\left[\sum \frac{r(t)}{Ew(t)} + C\right] = q^t w(1)\left[\sum \frac{Kt^n q^{t-1}}{q^{t+1}w(1)} + C\right] = Kq^{t-2}\left[\sum t^n + P\right] = Kq^{t-2}\left[\frac{1}{n+1}B_{n+1}(t) + P\right] \\ &= \frac{K}{1+n}B_{n+1}(t)q^{t-2} + PKq^{t-2}, \end{aligned}$$

where C is an arbitrary constant and $P = qw(1)C/K$. Notice that

$$\lim_{t\to\infty} PKq^{t-2} = 0 \quad \text{and} \quad \lim_{t\to\infty} \frac{K}{n+1}B_{n+1}(t)q^{t-2} = 0$$

(since $0 < q < 1$, B_n are Bernoulli polynomials, for all $n \in \mathbb{Z}_+ \cup \{0\}$, and because of L'Hôpital's rule applied $n+1$ times for the second limit). It follows that $\lim_{t\to\infty} z(t) = 0$. □

We can also prove that the type of function chosen for $r(t)$ in Lemma 4 satisfies

$$\lim_{t\to\infty} r(t) = \lim_{t\to\infty} Kt^n q^{t-1} = 0$$

for all $n \in \mathbb{Z}_+ \cup \{0\}$, by applying again L'Hôpital's rule n times.

Lemma 5. *Let $f(u_1, u_2) := u_1 u_2^2$ be defined over the set $S = \{(u_1, u_2)^{\mathrm{T}} \in \mathbb{R}^2 : 0 \leqslant |u_1| \leqslant \beta_1 \text{ and } 0 \leqslant |u_2| \leqslant \beta_2\}$. Then the function f satisfies Lipschitz condition on S with Lipschitz constant given by $L_0 := \beta_2\sqrt{\beta_1^2 + 4\beta_1}$. In other words, for every $(u_1, u_2)^{\mathrm{T}}, (v_1, v_2)^{\mathrm{T}} \in S$, we have*

$$|f(u_1, u_2) - f(v_1, v_2)| \leqslant L_0\|(u_1 - v_1, u_2 - v_2)\|.$$

Proof. Since the set S is compact and convex subset of $\mathbb{R}^2$ and f has continuous partial derivatives on S, we have, by the Mean Value Theorem [12], for some $\mathbf{c} = (c_1, c_2)^{\mathrm{T}}$ in the line segment joining $(u_1, u_2)^{\mathrm{T}}$ and $(v_1, v_2)^{\mathrm{T}}$ which lies entirely in S,

$$\begin{aligned} |f(u_1, u_2) - f(v_1, v_2)| &= \|\nabla f(\mathbf{c}) \cdot (u_1 - v_1, u_2 - v_2)\| \leqslant \|\nabla f(\mathbf{c})\|\|(u_1 - v_1, u_2 - v_2)\| \\ &= \|(c_2^2, 2c_1c_2)\|\|(u_1 - v_1, u_2 - v_2)\| = |c_2|\sqrt{c_2^2 + 4c_1^2}\|(u_1 - v_1, u_2 - v_2)\| \\ &\leqslant \beta_2\sqrt{\beta_2^2 + 4\beta_1^2}\|(u_1 - v_1, u_2 - v_2)\|, \end{aligned}$$

as required. □

We establish the following theorem which specifies the type of conditions required to guarantee the convergence of solutions of system (13) to zero as time approaches infinity.

Theorem 2. *Let q_k be the largest eigenvalue of $(I+Q_k)^{\mathrm{T}}(I+Q_k)$ and $\Delta_{k+1} := t_{k+1} - t_k \leqslant \Delta$, for all $k = 1,2,\ldots$ and for some $\Delta > 0$. In addition, let $q := \sup_k q_k$, $d = \max(d_1, d_2)$,*

$$\beta_i := \max\left(\sup_{t\in\mathbb{R}_+} u_i(t), \sup_{t\in\mathbb{R}_+} v_i(t)\right),$$

$$\mathscr{E}_i := \sup_{t\in\mathbb{R}_+}\left|\frac{\partial e_i}{\partial x}(t,L) - \frac{\partial e_i}{\partial x}(t,0)\right|$$

for $i = 1$ and 2,

$$\beta := 4\beta_2\sqrt{\beta_2^2 + 4\beta_1^2} - 2a,$$

$\mathscr{E} := \max(\mathscr{E}_1, \mathscr{E}_2)$ and $\mathscr{F} := 2d\mathscr{E}/\beta$. If $\widetilde{\mathbf{H}}(t) = (\widetilde{H}_1(t), \widetilde{H}_2(t))^{\mathrm{T}}$, $\widetilde{H}(t) := \widetilde{H}_1(t) + \widetilde{H}_2(t)$ with $\mathbf{g}(t) = (0.5, 0.5)^{\mathrm{T}}$, for all $t \in \mathbb{R}_+$ (i.e., $g_1(t) + g_2(t) = 1$), and

$$q\mathrm{e}^{\beta\Delta} < 1, \tag{14}$$

then system (13) is equi-attractive in the large.

Proof. The proof of this Theorem is similar to that of Theorem 1. Choose the Lyapunov function (or energy function) to be

$$V(\mathbf{e}(t,x)) := \int_0^L \mathbf{e}^{\mathrm{T}}(t,x)\mathbf{e}(t,x)\mathrm{d}x = \int_0^L (e_1^2(t,x) + e_2^2(t,x))\mathrm{d}x.$$

In this case, we have, by Eq. (13) and Lemma 5,

$$\begin{aligned}
D_t^+ V(\mathbf{e}) &= 2\int_0^L \left(e_1\frac{\partial e_1}{\partial t} + e_2\frac{\partial e_2}{\partial t}\right)\mathrm{d}x \\
&= 2\int_0^L \left[-(u_1u_2^2 - v_1v_2^2)e_1 - ae_1^2 + d_1e_1\frac{\partial^2 e_1}{\partial x^2} + (u_1u_2^2 - v_1v_2^2)e_2 - (a+b)e_2^2 + d_2e_2\frac{\partial^2 e_2}{\partial x^2}\right]\mathrm{d}x \\
&\leqslant 2\int_0^L \left[|u_1u_2^2 - v_1v_2^2\|e_1| + |u_1u_2^2 - v_1v_2^2\|e_2|\right]\mathrm{d}x + 2\int_0^L \left[-ae_1^2 - (a+b)e_2^2\right]\mathrm{d}x \\
&\quad + 2\int_0^L \left[d_1e_1\frac{\partial^2 e_1}{\partial x^2} + d_2e_2\frac{\partial^2 e_2}{\partial x^2}\right]\mathrm{d}x \\
&\leqslant 4\beta_2\sqrt{\beta_2^2 + 4\beta_1^2}\int_0^L \|\mathbf{e}\|^2\mathrm{d}x - 2\int_0^L \left[ae_1^2 + (a+b)e_2^2\right]\mathrm{d}x + 2\int_0^L \left[d_1e_1\frac{\partial^2 e_1}{\partial x^2} + d_2e_2\frac{\partial^2 e_2}{\partial x^2}\right]\mathrm{d}x \\
&\leqslant \left(4\beta_2\sqrt{\beta_2^2 + 4\beta_1^2} - 2a\right)\|\mathbf{e}\|_2^2 + 2\int_0^L \left[d_1e_1\frac{\partial^2 e_1}{\partial x^2} + d_2e_2\frac{\partial^2 e_2}{\partial x^2}\right]\mathrm{d}x.
\end{aligned}$$

Apply integration by parts to the second term in the later inequality, we get, for $i = 1$ and 2,

$$\int_0^L e_i\frac{\partial^2 e_i}{\partial x^2}\,\mathrm{d}x = e_i\frac{\partial e_i}{\partial x}\Big|_0^L - \int_0^L \left(\frac{\partial e_i}{\partial x}\right)^2\mathrm{d}x \leqslant \mathscr{E}_i\widetilde{H}_i(t) - \int_0^L \left(\frac{\partial e_i}{\partial x}\right)^2\mathrm{d}x.$$

Thus

$$D_t^+ V(\mathbf{e}) \leqslant \left(4\beta_2\sqrt{\beta_2^2 + 4\beta_1^2} - 2a\right)\|\mathbf{e}\|_2^2 + 2d_1\mathscr{E}_1\widetilde{H}_1(t) + 2d_2\mathscr{E}_2\widetilde{H}_2(t) - 2d\|\mathbf{e}_x\|_2^2.$$

However, $-2d\|\mathbf{e}_x\|_2^2 \leqslant 0$. Therefore we can conclude that

$$\begin{aligned}
D_t^+ V(\mathbf{e}) &\leqslant \left(4\beta_2\sqrt{\beta_2^2 + 4\beta_1^2} - 2a\right)\|\mathbf{e}\|_2^2 + 2d_1\mathscr{E}_1\widetilde{H}_1(t) + 2d_2\mathscr{E}_2\widetilde{H}_2(t) \\
&\iff D_t^+ V(\mathbf{e}) \leqslant \beta\|\mathbf{e}\|_2^2 + 2d\mathscr{E}\widetilde{H}(t) = \beta V(\mathbf{e}) + 2d\mathscr{E}\widetilde{H}(t) \iff D_t^+ V(\mathbf{e}) - \beta V(\mathbf{e}) \leqslant 2d\mathscr{E}\widetilde{H}(t).
\end{aligned}$$

By multiplying both sides of the later inequality by $e^{-\beta t}$, we obtain

$$e^{-\beta t}D_t^+V(\mathbf{e}) - \beta e^{-\beta t}V(\mathbf{e}) \leqslant 2d\mathscr{E}\widetilde{H}(t)e^{-\beta t} \Longleftrightarrow D_t^+\left[e^{-\beta t}V(\mathbf{e})\right] \leqslant 2d\mathscr{E}\widetilde{H}(t)e^{-\beta t}.$$

It implies, by the definition of $\widetilde{H}(t)$ and for every $t \in (t_k, t_{k+1}]$, that

$$\int_{t_k^+}^{t} D_s^+\left[e^{-\beta s}V(\mathbf{e})\right]ds \leqslant -\mathscr{F}e^{-\beta t}\widetilde{H}(t) + \mathscr{F}e^{-\beta t_k}\widetilde{H}(t).$$

Hence, for $t \in (t_k, t_{k+1}]$, we have

$$V(\mathbf{e}(t,x)) \leqslant e^{\beta\Delta_{k+1}}V(\mathbf{e}(t_k^+,x)) + \mathscr{F}(e^{\beta\Delta_{k+1}} - 1)\widetilde{H}(t) \tag{15}$$

and

$$V(\mathbf{e}(t_{k+1},x)) \leqslant e^{\beta\Delta_{k+1}}V(\mathbf{e}(t_k^+,x)) + \mathscr{F}(e^{\beta\Delta_{k+1}} - 1)\widetilde{H}(t). \tag{16}$$

On the other hand, for every $x \in [0, L]$ and every $k = 1, 2, \ldots$, we have, by the structure of the impulses given in system (13),

$$\begin{aligned}\mathbf{e}(t_k^+,x) = (I + Q_k)\mathbf{e}(t_k,x) &\Longleftrightarrow V(\mathbf{e}(t_k^+,x)) = \int_0^L \mathbf{e}^{\mathrm{T}}(t_k,x)(I + Q_k)^{\mathrm{T}}(I + Q_k)\mathbf{e}(t_k,x)dx\\ &\Longleftrightarrow V(\mathbf{e}(t_k^+,x)) \leqslant q_k\int_0^L \mathbf{e}^{\mathrm{T}}(t_k,x)\mathbf{e}(t_k,x)dx.\end{aligned}$$

i.e.,

$$V(\mathbf{e}(t_k^+,x)) \leqslant q_kV(\mathbf{e}(t_k,x)). \tag{17}$$

Substituting inequality (17) into inequalities (15) and (16), we obtain

$$V(\mathbf{e}(t,x)) \leqslant q_ke^{\beta\Delta_{k+1}}V(\mathbf{e}(t_k,x)) + \mathscr{F}(e^{\beta\Delta_{k+1}} - 1)\widetilde{H}(t) \tag{18}$$

and

$$V(\mathbf{e}(t_{k+1},x)) \leqslant q_ke^{\beta\Delta_{k+1}}V(\mathbf{e}(t_k,x)) + \mathscr{F}(e^{\beta\Delta_{k+1}} - 1)\widetilde{H}(t). \tag{19}$$

Let $V_k := V(\mathbf{e}(t_k,x))$, for every $k = 1, 2, \ldots$ In this case, we have, by inequality (19) and for every $k = 1, 2, \ldots$,

$$V_{k+1} \leqslant q_ke^{\beta\Delta_{k+1}}V_k + \mathscr{F}(e^{\beta\Delta_{k+1}} - 1)\widetilde{H}(t) \leqslant qe^{\beta\Delta}V_k + \mathscr{F}(e^{\beta\Delta} - 1)\widetilde{H}(t).$$

Since $q_k < q < 1$, for every $k = 1, 2, \ldots$, we may conclude that, for every $t \in (t_k, t_{k+1}]$,

$$\mathscr{F}(e^{\beta\Delta} - 1)\widetilde{H}(t) < \mathscr{F}q^{k-1}.$$

Hence

$$V_{k+1} \leqslant qe^{\beta\Delta}V_k + \mathscr{F}q^{k-1}. \tag{20}$$

Define $\mathscr{V}_1 := V_1$ and $\mathscr{V}_{k+1} := qe^{\beta\Delta}\mathscr{V}_k + \mathscr{F}q^{k-1}$, for $k = 1, 2, \ldots$ This implies, by inequality (20) and induction, that $V_k \leqslant \mathscr{V}_k$, for all $k = 1, 2, \ldots$ However, by Lemma 4 and inequality (14), we have $\lim_{k\to\infty}\mathscr{V}_k = 0$. i.e., $\lim_{k\to\infty}V_k = 0$. Therefore

$$\lim_{k\to\infty} V(\mathbf{e}(t_k,x)) = 0,$$

which, in turn, implies that, by inequality (18),

$$\lim_{t\to\infty} V(\mathbf{e}(t,x)) = 0.$$

In other words, solutions to system (13) are equi-attractive in the large, as required. □

Remarks 3 and 4, from the previous section characterizing the KS model, are also suitable for this model, especially Remark 3 which reflects the fact that the conditions stated in Theorem 2 are sufficient conditions but not necessary. In addition, we have the following three remarks.

Remark 5. The existence of the parameters $\mathscr{E}_i$, $i = 1, 2$, indicates that the solution surfaces of the impulsive Grey–Scott model are bounded and that the frequency of the oscillations of the solution surfaces, at the boundary, is also bounded (i.e., boundary oscillations of the solution surfaces do not increase with time). This is consistent with the properties of

the Grey–Scott model and the boundary conditions corresponding to it. Therefore the existence of the parameters $\mathscr{E}_1$ and $\mathscr{E}_2$ is guaranteed.

Remark 6. Theorem 2 can be extended to the two-dimensional Grey–Scott model described by system (9), although the theory is more complicated due to the use of double integrals for the evaluation of the Lyapunov functions (or energy functions).

Remark 7. Theorem 2 assures the existence of the matrices Q_k, $k = 1,2,\ldots$, which will guarantee the convergence of solutions of the error system (13) to the equilibrium solution. Obtaining an estimate on q is done numerically upon knowing the other parameters of the system. In this case, an approximation of the basin of attraction for Δ can be obtained with this numerical value of q.

We show now several numerical simulations to confirm the results obtained in Theorem 2. The numerical method applied in these simulations is the forward Euler integrations of the finite-difference equations. As in the simulations of system (10), the integration step size in these simulations is taken to be 0.01 s and the number of spatial points is taken to be 257. Moreover, the initial conditions in these simulations are taken to be $(u_{01}(x), u_{02}(x))^{\mathrm{T}} = (1,0)^{\mathrm{T}}$ with strong perturbations in the middle and $(v_{01}(x), v_{02}(x))^{\mathrm{T}} = (1,0)^{\mathrm{T}}$ as well but with significantly different perturbations in the middle from the transmitter system. The remaining parameters of the error system are the same as described for the simulations of system (10). If the impulse durations are taken to be $\Delta_k = \Delta = 0.1$ s, for all $k = 1,2,\ldots$, then the solutions converge to zero by choosing $Q_k = Q = -0.5I$, for all $k = 1,2,\ldots$ Fig. 10 shows the quick convergence of the error dynamics to zero in 0.9 s, which is consistent with that of Theorem 2. It should be mentioned that with the discretization chosen above and the theoretical model represented by Eq. (13), the impulses are applied at every discrete point in the spatial direction x at every t_k, $k = 1,2,\ldots$ In other words, in the numerical model shown here, the impulses are applied on the 257 discrete spatial points corresponding to every t_k, $k = 1,2,\ldots$ This explains the quick convergence of solutions to zero. However, in [21,22], it was observed (with an example) that the numerical model obtained from the discretization of systems (10) and (11) (and hence the error system Eq. (13)) impulsively synchronize without the need to drive all of the 257 spatial points. i.e., the synchronization of the discrete models approximating systems (10) and (11) synchronize even by driving much smaller number of points in the spatial direction for every t_k, $k = 1,2,\ldots$ We confirm this result by showing two different examples with the same value for Δ and Q. In the first example, we drive 32 spatial points in the e_1 and e_2 directions simultaneously, for every t_k, $k = 1,2,\ldots$ Fig. 11 shows how the error system converges to zero very slowly. In fact the convergence is significantly faster if the impulses are applied at the 32 spatial points but in the e_2 direction only (i.e., $Q = \mathrm{diag}(0,-0.5)$), as shown in Fig. 12. This is a significant difference between the theoretical model presented earlier and the numerical model shown in the simulations. The reason for the numerical models to show convergence is that the equations obtained by discretization are coupled equations. Thus if the impulse is applied at one particular discrete point, then the neighboring points are also affected because of the coupling factor. This does not hold in the theoretical (or continuous model), because impulses are applied in a continuous manner and it is impossible to apply impulses at discrete points (since the solutions, in this case, are hypersurfaces). In the next section, we shall explain the reasons behind the convergence behaviour in Figs. 11 and 12, by employing the *numerical method of lines*, for solving PDE's, and the Lyapunov exponents analysis.

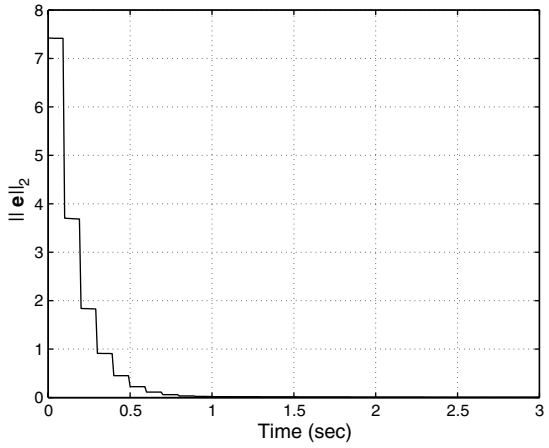

Fig. 10. $\|\mathbf{e}(t,x)\|_2$ converging to zero for $\Delta = 0.1$ and $Q_k = Q = -0.5I$.

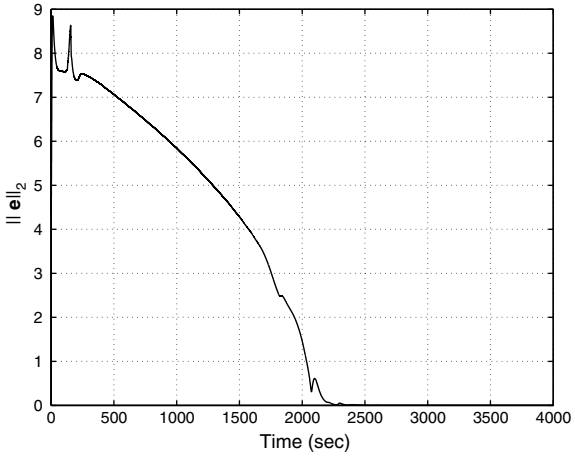

Fig. 11. $\|\mathbf{e}(t,x)\|_2$ converging to zero for $\Delta = 0.1$, and $Q_k = Q = -0.5I$ with impulses applied at 32 spatial points in the direction of e_1 and e_2.

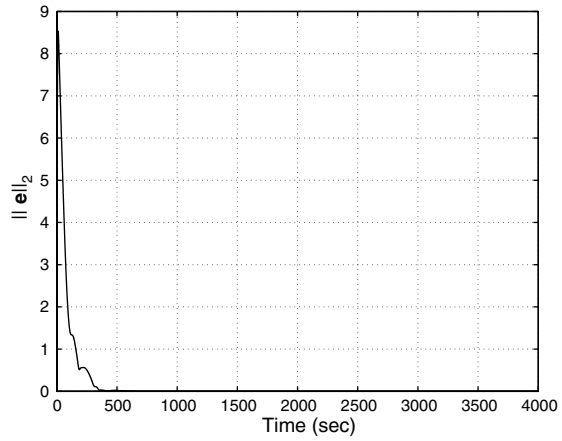

Fig. 12. $\|\mathbf{e}(t,x)\|_2$ converging to zero for $\Delta = 0.1$, and $Q_k = Q = \mathrm{diag}(0,-0.5)$ with impulses applied at 32 spatial points in the direction of e_2 only.

5. Lyapunov exponents analysis

We have developed in the previous section a scheme for impulsively synchronizing two Grey–Scott models. This was done by applying analytical methods which generated sufficient conditions on the impulses and on the parameters of the systems involved. Enforcing these conditions guarantees equi-attractivity in the large property of the error dynamics between the two Grey–Scott models. It remains to investigate how this method behaves when we analyze the error dynamics numerically. In other words, we need to check the Lyapunov exponents of the synchronization error systems developed in the previous section and see if the results are consistent with the theoretical results we have already obtained in Theorem 2. Due to the fact that impulsive systems have a unique character represented by jump discontinuities at the moments of impulse, the classical approach of finding Lyapunov exponents of the error dynamics is not applicable in this case. We shall, therefore, apply a different technique, proposed in [13], to study the dynamics of the synchronization error systems described by ODE's. However, in this section, we shall extend this technique to analyze the Lyapunov exponents of error dynamics between two identical spatiotemporal chaotic systems. Then we shall introduce an illustrative numerical example employing the Gray–Scott model to show how the technique works. The theory will depend on the *numerical method of lines* for PDE's to develop the technique.

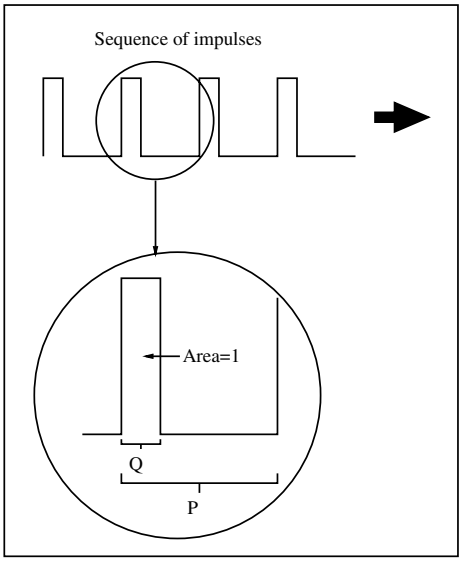

Fig. 13. A scheme showing the structure of the impulses.

We shall concern ourselves with unidirectional-coupling in impulsive synchronization. In other words, one system will impulsively drive the other but not vice versa. In a uni-coupled synchronization scheme, we transmit the impulses sampled from one state variable of the driving system to the response system (driven system). To avoid clutter, and without loss of generality, we study the case when impulse samples are equidistant. Let Δ and P denote the period and the width of the impulse samples, respectively. Note that Δ and P must satisfy $P \ll \Delta$ and the area enclosed by the impulse is equal to 1 (see Fig. 13). We begin our discussion by first dealing with the case when we have impulsive driving along the whole spatial direction x. i.e., using the discretization we mentioned in the previous section, where every discrete spatial point, at every moment t_k, $k = 0, 1, \ldots$, is driven. The set of matrices Q_k, $k = 0, 1, \ldots$, will be chosen to be

$$Q_k = \overline{Q} = \begin{pmatrix} -I & O_1 \\ O_2 & O_3 \end{pmatrix},$$

where I is an $\ell \times \ell$ identity matrix and O_1, O_2 and O_3 are the $\ell \times m$, $m \times \ell$ and $m \times m$ zero matrices, respectively ($\ell + m = n$). This motivates us to split the drive system into two dynamical models: one which corresponds to the period given by P and the other which corresponds to the period given by $\Delta - P$. Let $\mathbf{u} := (\mathbf{u}_1, \mathbf{u}_2)^{\mathrm{T}}$, where $\boldsymbol{u}_1 = (u_{11}, u_{12}, \ldots, u_{1\ell})^{\mathrm{T}}$ and $\boldsymbol{u}_2 = (u_{21}, u_{22}, \ldots, u_{2m})^{\mathrm{T}}$. In this case, the general form of the driving system will be given by

$$\begin{cases} \frac{\partial \mathbf{u}_1}{\partial t} = \mathbf{p}(\mathbf{u}_1, \mathbf{u}_2, \mathbf{u}_{1x}, \mathbf{u}_{2x}, \ldots), \\ \frac{\partial \mathbf{u}_2}{\partial t} = \mathbf{q}(\mathbf{u}_1, \mathbf{u}_2, \mathbf{u}_{1x}, \mathbf{u}_{2x}, \ldots), \end{cases} \tag{21}$$

where we have assumed that $\mathbf{p}$ and $\mathbf{q}$ are both independent of the time variable t and the spatial variable x, an assumption which is consistent with the models discussed in this paper. However, for the response system, we have two sets of time intervals to consider.

- For all $x \in [0, L]$ and for $t \in [k\Delta, k\Delta + P)$, $k = 0, 1, \ldots$, we have

$$\text{Response system A} \begin{cases} \mathbf{u}_1' = \mathbf{u}_1, \\ \frac{\partial \mathbf{u}_2'}{\partial t} = \mathbf{q}(\mathbf{u}_1, \mathbf{u}_2', \mathbf{u}_{1x}', \mathbf{u}_{2x}', \ldots). \end{cases} \tag{22}$$

- For all $x \in [0, L]$ and for $t \in [k\Delta + P, (k+1)\Delta)$, $k = 0, 1, \ldots$, we have

$$\text{Response system B} \begin{cases} \frac{\partial \mathbf{u}_1'}{\partial t} = \mathbf{p}(\mathbf{u}_1', \mathbf{u}_2', \mathbf{u}_{1x}', \mathbf{u}_{2x}', \ldots), \\ \frac{\partial \mathbf{u}_2'}{\partial t} = \mathbf{q}(\mathbf{u}_1', \mathbf{u}_2', \mathbf{u}_{1x}', \mathbf{u}_{2x}', \ldots). \end{cases} \tag{23}$$

It follows, from systems (22) and (23), that the synchronization error will be given by

- For response system A: with $x \in [0, L]$ and $t \in [k\Delta, k\Delta + P)$, $k = 0, 1, \ldots$, we have

$$\begin{cases} \mathbf{e}_1 = \mathbf{0}, \\ \frac{\partial \mathbf{e}_2}{\partial t} = \mathbf{q}(\mathbf{u}_1, \mathbf{u}_2, \mathbf{u}_{1x}, \mathbf{u}_{2x}, \ldots) - \mathbf{q}(\mathbf{u}_1, \mathbf{u}'_2, \mathbf{u}'_{1x}, \mathbf{u}'_{2x}, \ldots). \end{cases} \tag{24}$$

- For response system B: with $x \in [0, L]$ and $t \in [k\Delta + P, (k+1)\Delta)$, $k = 0, 1, \ldots$, we have

$$\begin{cases} \frac{\partial \mathbf{e}_1}{\partial t} = \mathbf{p}(\mathbf{u}_1, \mathbf{u}_2, \mathbf{u}_{1x}, \mathbf{u}_{2x}, \ldots) - \mathbf{p}(\mathbf{u}'_1, \mathbf{u}'_2, \mathbf{u}'_{1x}, \mathbf{u}'_{2x}, \ldots), \\ \frac{\partial \mathbf{e}_2}{\partial t} = \mathbf{q}(\mathbf{u}_1, \mathbf{u}_2, \mathbf{u}_{1x}, \mathbf{u}_{2x}, \ldots) - \mathbf{q}(\mathbf{u}'_1, \mathbf{u}'_2, \mathbf{u}'_{1x}, \mathbf{u}'_{2x}, \ldots). \end{cases} \tag{25}$$

Notice that systems (24) and (25) are partial differential equations. Therefore applying the same derivations given in [13] is not feasible even with use of the norm given in Definition 1. This is due to the presence of the spatial derivatives $\boldsymbol{u}_{ix}, \mathbf{u}_{ixx}, \ldots, i = 1, 2$. Therefore in order to implement the same techniques discussed in [13], we need to apply the *numerical method of lines* for integrating partial differential equations [33]. This method is based on transforming the spatial derivatives $\mathbf{u}_{ix}, \mathbf{u}_{ixx}, \ldots, i = 1, 2$, into finite difference expressions (discretization). In other words, systems (24) and (25) are transformed into a system of N ordinary differential equations, where N depends on the number of spatial points in the discretization process. The new system of ODE's, which approximates the dynamics of the system of PDE's, will be used to discuss the dynamics of the synchronization error. In this case, the synchronization error, $(\mathbf{e}_1, \mathbf{e}_2)^{\mathrm{T}}$, will be given by

- For response system A: with $t \in [k\Delta, k\Delta + P)$, $k = 0, 1, \ldots$, we have

$$\begin{cases} \mathbf{e}_1 = \mathbf{0}, \\ \dot{\mathbf{e}}_2 = \tilde{\mathbf{q}}(\mathbf{u}_1, \mathbf{u}_2) - \tilde{\mathbf{q}}(\mathbf{u}_1, \mathbf{u}'_2). \end{cases} \tag{26}$$

- For response system B: $t \in [k\Delta + P, (k+1)\Delta)$, $k = 0, 1, \ldots$, we have

$$\begin{cases} \dot{\mathbf{e}}_1 = \tilde{\mathbf{p}}(\mathbf{u}_1, \mathbf{u}_2) - \tilde{\mathbf{p}}(\mathbf{u}'_1, \mathbf{u}'_2), \\ \dot{\mathbf{e}}_2 = \tilde{\mathbf{q}}(\mathbf{u}_1, \mathbf{u}_2) - \tilde{\mathbf{q}}(\mathbf{u}'_1, \mathbf{u}'_2). \end{cases} \tag{27}$$

The equations in (26) and (27) are systems of ODE's that can be approximated by the variational systems, given by

$$\dot{\mathbf{e}} = J_{\mathbf{u}_1} \tilde{\mathbf{p}}(\mathbf{u}_1, \mathbf{u}_2) \mathbf{e}_1 \tag{28}$$

and

$$\begin{pmatrix} \dot{\mathbf{e}}_1 \\ \dot{\mathbf{e}}_2 \end{pmatrix} = \begin{pmatrix} J_{\mathbf{u}_1} \tilde{\mathbf{p}}(\mathbf{u}_1, \mathbf{u}_2) & J_{\mathbf{u}_2} \tilde{\mathbf{p}}(\mathbf{u}_1, \mathbf{u}_2) \\ J_{\mathbf{u}_1} \tilde{\mathbf{q}}(\mathbf{u}_1, \mathbf{u}_2) & J_{\mathbf{u}_2} \tilde{\mathbf{q}}(\mathbf{u}_1, \mathbf{u}_2) \end{pmatrix} \begin{pmatrix} \mathbf{e}_1 \\ \mathbf{e}_2 \end{pmatrix}, \tag{29}$$

respectively, where J stands for the Jacobian matrices of the corresponding functions $\tilde{\mathbf{p}}$ and $\tilde{\mathbf{q}}$. Hence if we let μ and λ be the largest Lyapunov exponents of systems (28) and (29), respectively, then the inequality

$$D := (\mu - \lambda)P + \lambda\Delta < 0,$$

represents a sufficient condition to guarantee synchronization (see [13]).

In order to illustrate how the numerical method of lines works and how to incorporate it with the theory of Lyapunov exponents, we shall take the synchronization error between two identical Grey–Scott models discussed in Section 4. Suppose that samples of the state variable u_2 are used to drive the state variable v_2 in the response system at the discrete moments t_k, $k = 0, 1, \ldots$, for all $x \in [0, L]$ (here $\ell = m = 1$). Obviously, the response system A_1, for $x \in [0, L]$ and $t \in [k\Delta, k\Delta + P)$, $k = 0, 1, \ldots$, is given by

$$\text{Response system } A_1 \begin{cases} \frac{\partial e_1}{\partial t} = -(a + u_2^2)e_1 + d_1 \frac{\partial^2 e_1}{\partial x^2}, \\ e_2 = 0. \end{cases} \tag{30}$$

Applying the finite difference method, to discretize the last term in the first equation of (30), and the periodic boundary conditions, we get, for $j = 1, 2, \ldots, 255$,

$$\dot{e}_1^{(j)} = -\left[a + \left(u_2^{(j)}\right)^2\right] e_1^{(j)} + d_1 \frac{e_1^{(j+1)} - 2e_1^{(j)} + e_1^{(j-1)}}{(\Delta x)^2},$$

where $\Delta x = L/256$ (here $N = 256$). The largest Lyapunov exponent of the latter model is given by $\mu = -0.80867$. To evaluate the second Lyapunov exponent λ, we need to consider the response system B, given by

$$\text{Response system B}\begin{cases}\dfrac{\partial e_1}{\partial t} = -(u_1u_2^2 - v_1v_2^2) - ae_1 + d_1\dfrac{\partial^2 e_1}{\partial x^2},\\ \dfrac{\partial e_2}{\partial t} = u_1u_2^2 - v_1v_2^2 - (a+b)e_2 + d_2\dfrac{\partial^2 e_2}{\partial x^2}.\end{cases} \tag{31}$$

With the applications of the finite difference method and the periodic boundary conditions, system (31) becomes, for $j = 1, 2, \ldots, 255$,

$$\begin{cases}\dot{e}_1^{(j)} = -\left[u_1^{(j)}\left(u_2^{(j)}\right)^2 - v_1^{(j)}\left(v_2^{(j)}\right)^2\right] - ae_1^{(j)} + d_1\dfrac{e_1^{(j+1)} - 2e_1^{(j)} + e_1^{(j-1)}}{(\Delta x)^2},\\ \dot{e}_2^{(j)} = u_1^{(j)}\left(u_2^{(j)}\right)^2 - v_1^{(j)}\left(v_2^{(j)}\right)^2 - (a+b)e_2^{(j)} + d_2\dfrac{e_2^{(j+1)} - 2e_2^{(j)} + e_2^{(j-1)}}{(\Delta x)^2}.\end{cases} \tag{32}$$

The variational equation of system (32) is given by

$$\begin{cases}\dot{e}_1^{(j)} = -\left[a + \left(u_2^{(j)}\right)^2\right]e_1^{(j)} - 2u_1^{(j)}u_2(j)e_2^{(j)} + d_1\dfrac{e_1^{(j+1)} - 2e_1^{(j)} + e_1^{(j-1)}}{(\Delta x)^2},\\ \dot{e}_2^{(j)} = \left(u_2^{(j)}\right)^2 e_1^{(j)} + (2u_1^{(j)}u_2(j) - a - b)e_2^{(j)} + d_2\dfrac{e_2^{(j+1)} - 2e_2^{(j)} + e_2^{(j-1)}}{(\Delta x)^2}.\end{cases} \tag{33}$$

The largest Lyapunov exponent of system (33) is given by $\lambda = 0.0023$. Using these values for μ and λ, one can give an estimate on the maximum impulse duration permissible to achieve synchronization, provided that a value for the impulse width P is chosen.

The analysis of the case when the impulses are not applied along the whole spatial dimension x, is still very similar to the above approach. It is done by applying the method of lines first to the PDE's involved in the model, and creating a system of ODE's which will be used to find the Lyapunov exponents of the synchronization error. In the previous section, we discussed one particular example employing two identical Grey–Scott models which was motivated by the work in [20–22]. In that example, the spatial derivatives in the two Grey–Scott models were discretized using the finite difference method and the resulting ODE's were integrated numerically using forward Euler integration. The number of spatial points in that discrete model was 257 points for each given time step τ_s, $s = 1, 2, \ldots$. The impulsive driving was done at 33 spatial points of the 257 spatial points generated from discretizing the state variable v_2. In other words, taking $K = L/32$, the values of the impulses were given by

$$v_2(t_k^+, \eta K) = v_2(t_k, \eta K) - \epsilon(u_2(t_k, \eta K) - v_2(t_k, \eta K)), \tag{34}$$

$k = 0, 1, \ldots$ and $\eta = 0, 1, \ldots, 32$. In the previous section, we showed, through numerical simulations, that the norm of the error dynamics between the two Grey–Scott models approached zero when $\epsilon = -0.5$. Now suppose that the value of $\epsilon = -1$ and the method of lines is applied instead. This means that the spatial derivatives are discretized using finite difference method and the Grey–Scott models are transformed into two systems of 2×257 ordinary differential equations. In this case, 33 equations out of each one of these two systems of ODE's will be synchronized impulsively using the impulses described by equation (34). In this case, the discretized systems at the transmitter and receiver will be given by

$$\begin{cases}\dot{u}_1^{(0)} = -u_1^{(0)}\left(u_2^{(0)}\right)^2 + a\left(1 - u_1^{(0)}\right) + d_1\dfrac{2u_1^{(0)} - 5u_1^{(1)} + 4u_1^{(2)} - u_1^{(3)}}{(\Delta x)^2},\\ \dot{u}_2^{(0)} = u_1^{(0)}\left(u_2^{(0)}\right)^2 - (a+b)u_2^{(0)} + d_2\dfrac{2u_2^{(0)} - 5u_2^{(1)} + 4u_2^{(2)} - u_2^{(3)}}{(\Delta x)^2},\\ \dot{u}_1^{(j)} = -u_1^{(j)}\left(u_2^{(j)}\right)^2 + a\left(1 - u_1^{(j)}\right) + d_1\dfrac{u_1^{(j+1)} - 2u_1^{(j)} + u_1^{(j-1)}}{(\Delta x)^2},\\ \dot{u}_2^{(j)} = u_1^{(j)}\left(u_2^{(j)}\right)^2 - (a+b)u_2^{(j)} + d_2\dfrac{u_2^{(j+1)} - 2u_2^{(j)} + u_2^{(j-1)}}{(\Delta x)^2},\\ \dot{u}_1^{(256)} = -u_1^{(256)}\left(u_2^{(256)}\right)^2 + a\left(1 - u_1^{(256)}\right) + d_1\dfrac{2u_1^{(256)} - 5u_1^{(255)} + 4u_1^{(254)} - u_1^{(253)}}{(\Delta x)^2},\\ \dot{u}_2^{(256)} = u_1^{(256)}\left(u_2^{(256)}\right)^2 - (a+b)u_2^{(256)} + d_2\dfrac{2u_2^{(256)} - 5u_2^{(255)} + 4u_2^{(254)} - u_2^{(253)}}{(\Delta x)^2}\end{cases} \tag{35}$$

at the transmitter end, whereas at the receiver end, we have

$$\begin{cases} \dot{v}_1^{(0)} = -v_1^{(0)}\left(v_2^{(0)}\right)^2 + a\left(1 - v_1^{(0)}\right) + d_1\dfrac{2v_1^{(0)} - 5v_1^{(1)} + 4v_1^{(2)} - v_1^{(3)}}{(\Delta x)^2}, \\ \dot{v}_2^{(0)} = v_1^{(0)}\left(v_2^{(0)}\right)^2 - (a+b)v_2^{(0)} + d_2\dfrac{2v_2^{(0)} - 5v_2^{(1)} + 4v_2^{(2)} - v_2^{(3)}}{(\Delta x)^2}, \\ \dot{v}_1^{(j)} = -v_1^{(j)}\left(v_2^{(j)}\right)^2 + a\left(1 - v_1^{(j)}\right) + d_1\dfrac{v_1^{(j+1)} - 2v_1^{(j)} + v_1^{(j-1)}}{(\Delta x)^2}, \\ \dot{v}_2^{(j)} = v_1^{(j)}\left(v_2^{(j)}\right)^2 - (a+b)v_2^{(j)} + d_2\dfrac{v_2^{(j+1)} - 2v_2^{(j)} + v_2^{(j-1)}}{(\Delta x)^2}, \\ \dot{v}_1^{(256)} = -v_1^{(256)}\left(v_2^{(256)}\right)^2 + a\left(1 - v_1^{(256)}\right) + d_1\dfrac{2v_1^{(256)} - 5v_1^{(255)} + 4v_1^{(254)} - v_1^{(253)}}{(\Delta x)^2}, \\ \dot{v}_2^{(256)} = v_1^{(256)}\left(v_2^{(256)}\right)^2 - (a+b)v_2^{(256)} + d_2\dfrac{2v_2^{(256)} - 5v_2^{(255)} + 4v_2^{(254)} - v_2^{(253)}}{(\Delta x)^2}, \\ v_2(t_k^+)^{(8*\eta)} = v_2(t_k)^{(8*\eta)} - \epsilon(u_2(t_k)^{(8*\eta)} - v_2(t_k)^{(8*\eta)}) \end{cases} \tag{36}$$

for $j = 1,2,\ldots,255$, for $\eta = 0,1,\ldots,32$. In other words, the new state variables $v_1^{(j)}$ and $v_2^{(j)}$ are impulsively synchronized with the state variables $u_1^{(j)}$ and $u_2^{(j)}$, for $j = 0,1,\ldots,256$, by impulsively driving $v_1^{(8*\eta)}$ and $v_2^{(8*\eta)}$ by the discrete values of $u_1^{(8*\eta)}$ and $u_2^{(8*\eta)}$, $\eta = 0,1,\ldots,32$, at the moments t_k, $k = 1,2,\ldots$ If we denote the vector $(u_1^{(0)}, u_1^{(8)}, u_1^{(16)}, \ldots, u_1^{(256)})$ by $\bar{\mathbf{x}}$ and the vector consisting of the remaining state variables at the transmitter end by $\bar{\mathbf{y}}$, whereas we denote the vector $(v_1^{(0)}, v_1^{(8)}, v_1^{(16)}, \ldots, v_1^{(256)})$ by $\bar{\mathbf{x}}'$ and the vector consisting of the remaining state variables at the receiver end by $\bar{\mathbf{y}}'$, then the theory developed in [13] becomes once more applicable. Thus a typical expression for the response system A_2, for $t \in [k\Delta, k\Delta + P)$, $k = 0,1,\ldots$, will be given by

$$\begin{cases} \bar{\mathbf{X}} := \bar{\mathbf{x}} - \bar{\mathbf{x}}' = 0, \\ \dot{\bar{\mathbf{Y}}} := \dot{\bar{\mathbf{y}}} - \dot{\bar{\mathbf{y}}}'. \end{cases} \tag{37}$$

The variational equation approximating the error dynamics given by (37) can be evaluated and a fourth order Runge–Kutta method may be used to integrate the resulting variational equation in order to find its largest Lyapunov exponent. By applying Matlab programming, we found out that the largest Lyapunov exponent of system (37) is given by $\mu = -0.0242$. Unlike the latter description, when $t \in [k\Delta + P, (k+1)\Delta)$, $k = 0,1,\ldots$, (i.e., outside the impulse), the response system will be identical to the response system B obtained in the previous example. Thus the error dynamics between the ODE's at the transmitter and receiver are identical to those given by Eq. (32). This means that the value of $\lambda = 0.0023$.

Once more, knowing these values of μ and λ, one may obtain an upper bound on the maximum impulse duration permissible to achieve synchronization provided that P, the width of the impulse, is known.

6. Conclusion

We have shown that the impulsive control of the solution trajectories of the Kuramoto–Sivashinsky equation and the impulsive synchronization of two identical Grey–Scott models can be achieved by applying certain kind of impulses. This is a generalization of the theory of impulsive control from ODE's to PDE's. Since PDE's, which generate spatiotemporal chaos, have more complex dynamics in comparison with ODE's, it is expected that the impulsive control and synchronization of spatiotemporal chaos will have promising applications towards secure communication.

Acknowledgements

This work was supported by the Ontario Graduate Scholarship Program and partially by the Natural Sciences and Engineering Research Council of Canada.

References

[1] Bainov D, Kamont Z, Minchev E. On the impulsive partial differential-functional inequalities of first order. Util Math 1995;48:107–28.
[2] Bainov D, Kamont Z, Minchev E. On the stability of solutions of impulsive partial differential equations of first order. Adv Math Sci Appl 1996;6(2):589–98.
[3] Bainov D, Minchev E. On the stability of solutions of impulsive partial differential-functional equations of first order via Lyapunov functions. Non-Linear Phenom Complex Syst 2000;30(2):109–16.
[4] Boccaletti S, Bragard J, Arecchi FT. Controlling and synchronizing space time chaos. Phys Rev E 1999;59(6):6574–8.
[5] Boccaletti B, Bragard J, Arecchi FT, Mancini H. Synchronization in non-identical extended systems. Phys Rev Lett 1999;83(3):536–9.
[6] Cross MC, Hohenberg PC. Pattern formation outside of equilibrium. Rev Mod Phy 1993;65(8):851–1112.
[7] Erbe LH, Freedman HI, Liu XZ, Wu JH. Comparison principles for impulsive parabolic equations with applications to models of single species growth. J Austral Math Soc Ser B 1991;32:382–400.
[8] Franceschini G, Bose S, Schöll E. Control of chaotic spatiotemporal spiking by time-delay auto-synchronization. Phys Rev E 1999;60(5):5426–34.
[9] Fraser B, Yu P, Lookman T. Secure communications using chaos synchronization. Phys Canada, Special Issue on Non-Linear Dynam 2001;57(2):155–61.
[10] García-Ojalvo J, Roy R. Parallel communication with optical spatiotemporal chaos. IEEE Trans Circuits Syst I 2001;48(12):1491–7.
[11] García-Ojalvo J, Roy R. Spatiotemporal communication with synchronized optical chaos. Phys Rev lett 2001;86:5204–7.
[12] Hurley JF. Multivariable calculus. Philadelphia: Saunders College Publishing; 1981.
[13] Itoh M, Yang T, Chua LO. Conditions for impulsive synchronization of chaotic and hyperchaotic systems. Int J Bifurcat Chaos 2001;11(2):551–60.
[14] Junge L, Parlitz U. Control and synchronization of spatially extended systems. NOLTA'98, Le Régent, Crans-Montana, Switzerland. p. 303–6.
[15] Junge L, Parlitz U. Synchronization and control of coupled Ginzburg–Landau equations using local coupling. Phys Rev E 2000;61(4):3736–42.
[16] Junge L, Parlitz U. Phase synchronization of coupled Ginzburg–Landau equations. Phys Rev E 2000;62(1):438–41.
[17] Junge L, Parlitz U, Tasev Z, Kocarev L. Synchronization and control of spatially extended systems using sensor coupling. Int J Bifurcat Chaos 1999;9(12):2265–70.
[18] Kamont Z, Zubic-Kowal B. Numerical methods for impulsive partial differential equations. Dynam Syst Appl 1998;7:29–52.
[19] Kelley WG, Peterson AC. Difference equations: an introduction with applications. 2nd ed. Academic Press; 2001.
[20] Kocarev L, Parlitz U. Synchronizing spatiotemporal chaos in coupled non-linear oscillators. Phys Rev Lett 1996;77(11):2206–9.
[21] Kocarev L, Tasev Z, Parlitz U. Synchronizing spatiotemporal chaos of partial differential equations. Phys Rev Lett 1997;79(1):51–4.
[22] Kocarev L, Tasev Z, Stojanovski T, Parlitz U. Synchronizing spatiotemporal chaos. Chaos 1997;7(4):635–43.
[23] Lakshmikantham V, Bainov DD, Simeonov PS. Theory of impulsive differential equations. Singapore: World Scientific; 1989.
[24] Lakshmikantham V, Liu XZ. Stability analysis in terms of two measures. Singapore: World Scientific; 1993.
[25] LeVeque RJ. Numerical methods for conservation laws. Basel: Birkhäuser Verlag; 1990.
[26] LeVeque RJ. Finite volume methods for hyperbolic problems. Cambridge University Press; 2002.
[27] Li ZG, Wen CY, Soh YC, Xie WX. The stabilization and synchronization of Chua's oscillators via impulsive control. IEEE Trans Circuits Syst I 2001;48(11):1351–5.
[28] Liu XZ. Stability results for impulsive differential systems with applications to population growth models. Dynam Stabil Syst 1994;9(2):163–74.
[29] Liu XZ. Impulsive stabilization and control of chaotic systems. Non-Linear Anal 2001;47:1081–92.
[30] Liu XZ, Willms AR. Impulsive controllability of linear dynamical systems with applications to maneuvers of spacecraft. MPE 1996;2:277–99.
[31] Liu XZ, Xu DY. Uniform asymptotic stability of abstract functional differential equations. J Math Anal Appl 1997;216:626–43.
[32] Pearson JE. Complex patters in a simple system. Science 1993;261:189–92.
[33] Schiesser WE. The numerical method of lines: integration of partial differential equations. Academic Press Inc; 1991.
[34] Stojanovski T, Kocarev L, Parlitz U. Driving and synchronizing by chaotic impulses. Phys Rev E 1996;43(9):782–5.
[35] Straughan B. The energy method, stability, and non-linear convection. New York: Springer-Verlag Inc; 1992.
[36] Tasev Z, Kocarev L, Junge L, Parlitz U. Synchronization of Kuramoto–Sivashinsky equations using spatially local coupling. Int J Bifurcat Chaos 2000;10(4):869–73.
[37] Xiao JH, Hu G, Qu Z. Synchronization of spatiotemporal chaos and its application to multichannel spread-spectrum communication. Phys Rev Lett 1996;11(20):4162–5.
[38] Yang T. In: Impulsive control theory. Lecture notes in control and information sciences, vol. 272. Berlin: Springer-Verlag; 2001.
[39] Yang T. Impulsive systems and control: theory and applications. Huntington, New York: Nova Science Publishers, Inc.; 2001.
[40] Yang T, Chua LO. Impulsive stabilization for control and synchronization of chaotic systems: theory and application to secure communication. IEEE Trans Circuits Syst I 1997;44(10):976–88.

[41] Yang T, Chua LO. Impulsive control and synchronization of non-linear dynamical systems and application to secure communication. Int J Bifurcat Chaos 1997;7(3):645–64.
[42] Yang T, Suykens JA, Chua LO. Impulsive control of non-autonomous chaotic systems using practical stabilization. Int J Bifurcat Chaos 1998;8(7):1557–64.
[43] Yang T, Yang CM, Yang LB. Control of Rössler system to periodic motions using impulsive control methods. Phys Lett A 1997;232:356–61.
[44] Yang T, Yang LB, Yang CM. Impulsive synchronization of Lorenz systems. Phys Lett A 1997;226(6):349–54.
[45] Yang T, Yang LB, Yang CM. Impulsive control of Lorenz system. Phys D 1997;110:18–24.